Inorg. Chem. **2002**, *41*, 709–714

X-ray Single-Crystal Structure and Magnetic Properties of $Fe[CH_3PO_3)]\cdot H_2O$: A Layered Weak Ferromagnet

Carlo Bellitto* and Fulvio Federici

CNR-Istituto di Chimica dei Materiali, Via Salaria Km. 29.5, C.P.10, I-00016 Monterotondo Staz. (Roma), Italy

Marcello Colapietro,* Gustavo Portalone, and Daniela Caschera

Università di Roma "La Sapienza", Dipartimento di Chimica, P.le A Moro, I-00185 Roma, Italy

Received July 5, 2001

The crystal and molecular structure of the layered weak-ferromagnet $Fe[CH_3PO_3]\cdot H_2O$ has been solved by X-ray single-crystal diffraction techniques. Crystal data for $Fe[CH_3PO_3]\cdot H_2O$ are the following: orthorhombic space group $Pna2_1$; a =17.538(2), b = 4.814(1), c = 5.719(1) Å. The structure is lamellar, and it consists of alternating organic and inorganic layers along the *a* direction of the unit cell. The inorganic layers are made of Fe(II) ions octahedrally coordinated by five phosphonate oxygen atoms and one from oxygen of the water molecule. Each phosphonate group coordinates four metal ions, through chelation and bridging, making in this way a cross-linked Fe–O network. The resultant layers are then separated by bilayers of the methyl groups, with van der Waals contacts between them. The compound is air stable, and it dehydrates under inert atmosphere at temperatures above 120 °C. The oxidation state of the metal ion is +2, and the electronic configuration is d^6 high spin (S = 2), as determined from dc magnetic susceptibility measurements from 150 K to ambient temperature. Below 100 K, the magnetic moment of $Fe[CH_3PO_3]\cdot H_2O$ rises rapidly to a maximum at $T_{max} \cong$ 24 K, and then it decreases again. The onset of peak at T = 25 K is associated with the 3D antiferromagnetic long-range ordering, T_N. The observed critical temperature, T_N, is like all the other previously reported Fe(II) phosphonates, and it appears to be nearly independent of the interlayer spacing in this family of hybrid organic–inorganic layered compounds. Below T_N, the compound behaves as a "*weak ferromagnet*", and represents the third kind of magnetic materials with a spontaneous magnetization below a finite critical temperature, ferromagnets and ferrimagnets being the other two types.

Introduction

Metal(II) phosphonates, $M[RPO_3]\cdot H_2O$, and bis(phosphonates), $M_2[O_3P\text{-}R\text{-}PO_3]\cdot 2H_2O$ (M = divalent metal ion; R = alkyl or aryl group)[1−3] provide interesting examples of hybrid organic−inorganic solids. They, in fact, crystallize often in a lamellar structure, where inorganic and organic layers alternate along one direction of the unit cell. The metal ions are six-coordinated by five oxygens of the phosphonate groups and one from the water molecule. Since the compound contains only 1 phosphonate/metal ion, all the phosphonate oxygens take part in the metal binding and two oxygens chelate the metal ion and, at the same time, bridge across adjacent metal atoms in the same row. The oxygens are three-coordinate, and the third oxygen of the phosphonate ligand bridges to the adjacent row, thus creating the layer arrangement. This kind of coordination generates a *kinked* layer. The inorganic layer is then separated one from the other by the layers made of the organic part of the ligand. This implies that by increasing the number of carbon atoms of the ligand, it is possible to increase the interlayer distance in the mentioned systems and therefore the thickness of the organic layers. The inorganic layer, which mimics the metal oxide layers, is then well separated from the others by the organic layer, thus reducing the magnetic interactions along the third direction of the lattice. The *two-dimensional* lattice

* Corresponding authors. E-mail (C.B.): carlo@mlib.cnr.it.

(1) Alberti, G. In *Comprehensive Supramolecular Chemistry*; Lehn, J. M., Ed.; Pergamon Press: London, 1996; Vol. 7.
(2) Clearfield, A. *Prog. Inorg. Chem.* **1998**, *47*, 371.
(3) (a) Cao, G.; Lee, H.; Lynch, V. M.; Mallouck, T. E *Inorg. Chem.* **1988**, *27*, 2781. (b) Cao, G.; Lee, H.; Lynch, V. M.; Yacullo, L. M. *Chem. Mater.* **1993**, *5*, 1000. (c) Martin, K. J.; Squattrito, P. J.; Clearfield, A. *Inorg. Chim. Acta* **1989**, *7−9*, 7.

10.1021/ic0107126 CCC: $22.00
Published on Web 01/25/2002

favors the next-neighbors exchange magnetic interactions in phosphonates containing paramagnetic ions, and a long-range magnetic ordering has been observed at low temperatures.[4,5] We have recently prepared and studied the magnetic properties of $Cr[CH_3PO_3]\cdot H_2O$,[5] $Fe_2[O_3P(CH_2)_2PO_3]\cdot 2H_2O$,[6] and of $Fe[C_6H_5PO_3]\cdot H_2O$,[7] and we have found that they show all 3D antiferromagnetic order at low temperatures. But, below the ordering temperature, T_N, the equilibrium distribution of moments is not collinear; it is "*canted*" giving rise to a spontaneous magnetization. The existence of the hysteresis loop, below the critical temperature, confers a memory effect on the material. This phenomenon is known as *canted antiferromagnetism* or *weak ferromagnetism*.[8] The crystal structures of metal(II) phosphonates were mainly solved from X-ray powder diffraction studies, because they are very often isolated as a microcrystalline powder. Only a few metal(II) phosphonate structures have been refined from X-ray single-crystal data,[3] and only one for the iron(II) derivatives, i.e. $Fe[C_2H_5PO_3]\cdot H_2O$, has been reported.[9] With the aim at studying the correlation between the crystal structure and the magnetic properties of these hybrid organic−inorganic magnetic solids, we have grown single crystals of $Fe[CH_3PO_3]\cdot H_2O$, the first member of the series.

This paper deals with the crystal growth, X-ray single-crystal and molecular structure, and magnetic studies of Fe(II) methylphosphonate. Preliminary results were reported previously.[6]

Experimental Section

Materials and Methods. Methylphosphonic acid, $CH_3PO_3H_2$, was of analytical grade (Aldrich Chemical Co.) and used without further purification. HPLC water was used as solvent. All reactions involving Fe(II) ion were carried out under inert atmosphere, using the usual Schlenck techniques. Elemental analyses were performed by Malissa and Reuter Mikroanalytische Laboratorien, Elbach, Germany. The UV−visible diffuse reflectance spectra were recorded on a Cary 5 spectrophotometer. Static magnetic susceptibility measurements were performed by using a Quantum Design MPMS5 SQUID magnetometer in fields up to 4 T. A cellulose capsule was filled with freshly prepared polycrystalline sample and placed in a polyethylene straw fixed at the end of a sample road. All the experimental data were corrected for the core magnetization using Pascal constants.

Synthesis and Crystal Growth of $Fe[CH_3PO_3]\cdot H_2O$. $[FeSO_4]\cdot 7H_2O$ (7 g, 25.18 mmol) was dissolved in 30 mL of water. The solution was added to a filtered clean aqueous solution containing methylphosphonic acid (2.70 g, 28.1 mmol) and urea (3.00 g, 50 mmol). The resulting colorless solution was heated under nitrogen at 90 °C for 1 week. The coulorless needlelike microcrystalline powder was separated from the solution, washed with water, and dried under vacuum at room temperature. The compound is stable to the air.

The growth of a suitable single crystal was carried out by heating to 90 °C for about 2 weeks a sealed ampule containing a degassed water solution (30 mL) of $[FeSO_4]\cdot 7H_2O$ (1.33 g, 4.8 mmol), $CH_3PO_3H_2$ (0.51 g, 5.3 mmol), and urea (0.51 g, 8.5 mmol). Colorless platelets were collected, filtered out, and dried to the air.

Anal. Calcd for $Fe[CH_3PO_3]\cdot H_2O$: Fe, 33.27; C, 7.15; H, 3.00; P, 18.45; O, 28.6. Found: Fe, 34.05; C, 7.18; H, 2.97; P, 17.37.

X-ray Crystal Structure Analysis. The crystal used for the X-ray diffraction studies was a colorless platelet of dimensions 0.20 × 0.20 × 0.10 mm^3. Details of the crystal data, data collection, structure solution, and refinement are reported in Table 1. Data were collected on a Huber CS diffractometer,[10] with graphite-monochromatized Mo Kα radiation (λ = 0.710 69 Å), using ω-scans. The crystal used for diffraction studies showed no decomposition during data collection. The data were corrected for *Lp* and for absorption, and the structure was solved by direct methods and refined by least-squares method using the SIR-CAOS package.[11a,b] All the hydrogen atoms, except those of the water molecule, were clearly located through a Fourier synthesis and

Table 1. Crystallographic Data for $Fe[CH_3PO_3]\cdot H_2O$

(a) Crystal Data	
empirical formula	FeO_4PCH_5
habit, color	platelets, white
cryst size (mm)	0.20 × 0.20 × 0.10
fw	167.87
cryst system	orthorhombic
space group	$Pna2_1$ (No. 33)
a (Å)	17.538(2)
b (Å)	4.814(1)
c (Å)	5.719(1)
V (Å^3)	482.8(2)
Z	4
D_m (g/cm^3)	2.06
D_c (g/cm^3)	2.31
T (K)	293
radiation (Å)	Mo Kα (λ = 0.710 69)
2θ range (deg)	2−60
h, k, l collcd	±24, 0−6, ±8
μ (cm^{-1})	33,507
reflcns collcd	2156
unique reflcns with $I \geq 2\sigma\|I\|$	603
(b) Structure Solution and Refinement	
refinement	$\|F_o\|$
soln method	direct methods
quantity minimized	$\sum w(F_o - F_c)^2$
weighting scheme: $1/(a + b\|F_o\| + c\|F_o\|^2)$	1.314 53, 0.090 82, 0.001 25
no. of params refined	63
$R(F)^a$	0.0363
$R_w(F)^b$	0.052
R_{int}	0.018
goodness of fit	0.985

$^a R(F) = \sum(|F_o| - |F_c|)/\sum|F_o|$. $^b R_w(F) = \sum w(|F_o| - |F_c|)^2/\sum w|F_o|^2$.

(4) Carling, S. G.; Day, P.; Visser, D.; Kremer, R. K. *J. Solid State Chem*. **1993**, *106*, 111.

(5) (a) Bellitto, C.; Federici, F.; Ibrahim, S. A. *J. Chem. Soc., Chem. Commun*. **1996**, 759. (b) Bellitto, C.; Federici, F.; Ibrahim, S. A. *Chem. Mater*. **1998**, *10*, 1076.

(6) Bellitto, C.; Federici, F.; Ibrahim, S. A.; Mahmoud, M. R. *Mater. Res. Soc. Symp. Proc*. **1999**, *547*, 487. (b) Altomare, A.; Bellitto, C.; Ibrahim, S. A.; Mahmoud, R. F.; Rizzi, R. *J. Chem. Soc., Dalton Trans*. **2000**, 3913.

(7) Altomare, A.; Bellitto, C.; Ibrahim, S. A.; Rizzi, R. *Inorg. Chem*. **2000**, *39*, 1803.

(8) See for example: Carlin, R. L. *Magnetochemistry*; Springer-Verlag: Berlin, 1986; p 149. (b) Moriya, T. *Phys. Rev*. **1960**, *120*, 91. (c) Shull, C. G.; Stranser, W. A.; Wollan, E. O. *Phys. Rev*. **1951**, *83*, 333.

(9) (a) Bujoli, B.; Pena, O.; Palvadeau, P.; Le Bideau, J.; Payen, C.; Rouxel, J. *Chem. Mater*. **1993**, *5*, 583. (b) Le Bideau, J.; Payen, C.; Bujoli, B.; Palvadeau, P.; Rouxel, J. *J. Magn. Magn. Mater*. **1995**, *140*, 1719.

(10) Colapietro, M.; Cappuccio, G.; Marciante, C.; Pifferi, A.; Spagna, R.; Helliwell, J. R. *J. Appl. Crystallogr*. **1992**, *25*, 192.

(11) (a) Burla, M. C.; Camalli, M.; Cascarano, G.; Giacovazzo, C.; Polidori, G.; Spagna, R.; Viterbo, D. *J. Appl. Crystallogr*. **1989**, *22*, 389. (b) Camalli, M.; Capitani, D.; Cascarano, G.; Giacovazzo, C.; Spagna, R. Italian Patent No. 3540 c/86; *SIR-CAOS user guide*; Istituto di Strutturistica Chimica CNR: Rome, Italy. (c) Nardelli, M. *Comput. Chem*. **1983**, *7*, 95.

introduced into the final least-squares refinement with isotropic temperature factors arbitrarily fixed to the corresponding value of their bonded atoms. All final calculations were done with PARST package.[11c]

Room-temperature X-ray powder diffraction data were recorded on a Seifert XRD-3000 diffractometer, Bragg−Brentano geometry, equipped with a curved graphite monochromator [λ(Cu Kα) = 1.540 56 Å] and a scintillation detector. The data were collected with a step size of 0.02° in 2θ and at count time of 4 s/step of 0.2° min^{-1} over the range 4° < 2θ < 80°. The sample was mounted on a glass flat plate, giving rising to a strong preferred orientation. The diffractometer zero point was determined from an external Si standard. The powder patterns were indexed by using a Seifert indexing program with the following unit-cell parameters: a = 17.50(1) Å; b = 4.82(1) Å; c = 5.72(1) Å. These data confirmed that the microcrystalline powder and the single crystals were identical. The unit-cell parameters and the space group $Pna2_1$ (see below) suggest the compound is isomorphous to $Cd[CH_3PO_3]\cdot H_2O$.[3b]

Optical Properties. The IR spectrum of $Fe[CH_3PO_3]\cdot H_2O$ is similar to those reported for other layered metal(II) phosphonates.[6] It features two intense and sharp bands centered at 3420 and 3470 cm^{-1}, assigned as OH stretching vibrations of coordinated water molecules. The band observed at 1610 cm^{-1} is assigned to the H_2O bending vibration. Two intense bands due to the $-PO_3$ group vibrations are observed in the range 1200−970 cm^{-1}. The complete deprotonation of the acid in the Fe(II) salt is confirmed by the absence of the −OH stretching vibrations of −POH at 2700−2550 and 2350−2100 cm^{-1}. Two small overtones are observed at 2923 and 2970 cm^{-1} and are due to $-CH_3$ group.

The optical spectrum in the NIR−visible region is similar to that observed for $[Fe(H_2O)_6]^{2+}$, where only the spin-allowed $^5T_{2g} \rightarrow {}^5E_g$ is expected.[12] The absorption spectra consist of two broad peaks, centered at 9.3 × 10^3 cm^{-1}, and another peak, even broader, at 6.25 × 10^3 cm^{-1}, probably due to a low-symmetry ligand-field component, which lifts the two-orbital degeneracy of the ^5E_g term.

Results

$Fe[CH_3PO_3]\cdot H_2O$ was prepared by refluxing $[FeSO_4]\cdot 7H_2O$ and a methylphosphonate in water, in the presence of urea at temperatures slightly above 80 °C, under inert atmosphere. Urea is highly soluble in water, and it decomposes by hydrolysis to $(NH_4)_2CO_3$. The rate of hydrolysis increases significantly at temperatures above 90 °C.[13] The hydrolysis of ammonium to ammonia and carbonate to hydrogen carbonate increases the pH. Under these conditions the deprotonated acid is present in solution, thus favoring the complexation of the metal ions and the precipitation of solid. The compound was isolated as a white air-stable microcrystalline solid. The purities of samples were checked by elemental analyses, X-ray powder diffraction, and TGA techniques. Single crystals were grown by heating slowly to 90 °C a sealed ampule containing a degassed water solution of the $[FeSO_4]\cdot 7H_2O$, the phosphonic acid, and urea.

Crystal and Molecular Structure. Positional and thermal parameters of atoms of the asymmetric unit are included in the Supporting Information. Selected bond lengths and bond angles are given in Table 2. Figure 1 shows the asymmetric unit and the numbering scheme used in the tables. The iron atoms are six-coordinated by five oxygens of the phosphonate groups, O(1), O(2), and O(3), of different asymmetric units and one from the water molecule, O(w). The [FeO_6] octahedron is distorted, and the Fe−O distances are slightly shorter than those observed in $Fe[C_2H_5PO_3]\cdot H_2O$, the only previously reported crystal structure.[9] The crystal packing of the compound along the *c* axis is shown in Figure 2. Since the compound contains only one phosphonate per metal ion, all the phosphonate oxygen atoms take part in metal binding and two oxygens, O(1) and O(2), chelate the metal ion and, at the same time, bridge across adjacent metal ions in the same row. Oxygens O(3) of the phosphonate lying in the mirror plane bonds to only one Fe atom, and it is located *trans* to the oxygen O(w) of the water molecule. The octahedron is distorted. One of the *cis* O−Fe−O angles that is subtended by the longer Fe−O bond lengths is small (∼66°), and the others range between 84 and 97°. Iron atoms are linked along *b* axis by the third oxygen of the phospho-

Table 2. Selected Bond Lengths (Å) and Angles (deg) for Non-Hydrogen Atoms for $Fe[CH_3PO_3]H_2O$ with Esd's in Parentheses as Units on the Last Digit

$Fe-O_1{}^a$	2.103(4)	$Fe-O_1{}^c$	2.250(2)
$Fe-O_2$	2.049(12)	$Fe-O_2{}^c$	2.266(4)
$Fe-O_3{}^b$	2.105(5)	$Fe-O_w$	2.196(4)
P−C	1.781(6)	$P-O_1$	1.485(13)
$P-O_2$	1.601(13)	$P-O_3$	1.517(4)
$O_1{}^a-Fe-O_w$	91.0(7)	$O_3{}^b-Fe-O_w$	173.9(1)
$O_1{}^c-Fe-O_w$	89.1(7)	$Fe^d-O_1-Fe^e$	119.6(5)
$O_1{}^c-Fe-O_2$	98.0(9)	$Fe-O_2-Fe^e$	121.3(3)
$O_1{}^c-Fe-O_2{}^c$	65.6(1)	Fe^d-O_1-P	127.1(4)
$O_1{}^a-Fe-O_2$	104.1(8)	$Fe-O_2-P$	92.8(4)
$O_1{}^a-Fe-O_2{}^c$	92.3(2)	$C-P-O_1$	111.1(7)
$O_1{}^a-Fe-O_1{}^c$	157.9(7)	$C-P-O_2$	106.0(7)
$O_2-Fe-O_2{}^c$	163.4(1)	$C-P-O_3$	109.0(2)
O_2-Fe-O_w	91.4(4)	O_1-P-O_2	104.8(7)
$O_2{}^c-Fe-O_w$	90.5(6)	O_1-P-O_3	112.4(4)
$O_1{}^a-Fe-O_3{}^b$	93.7(8)	O_2-P-O_3	113.4(4)
$O_1{}^c-Fe-O_3{}^b$	84.8(8)	Fe^d-O_3-P	131.5(1)
$O_2-Fe-O_3{}^b$	92.3(3)	Fe^c-O_1-P	96.5(3)
$O_2{}^c-Fe-O_3{}^b$	84.3(3)	$Fe-O_2-P$	124.0(7)

[a] $x, y, z + 1$. [b] $-x + 3/2, y - 1/2, z + 1/2$. [c] $-x + 3/2, y + 1/2, z + 1/2$. [d] $x, y, z - 1$. [e] $-x + 3/2, y - 1/2, z - 1/2$.

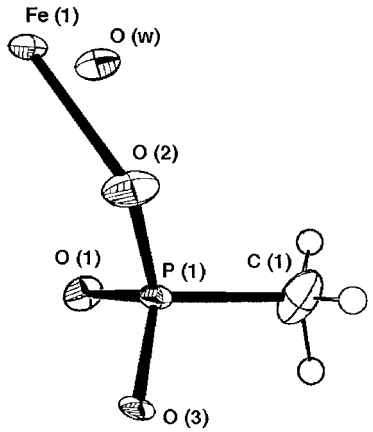

Figure 1. Schematic representation of the $Fe[CH_3PO_3]\cdot H_2O$ molecule, showing the asymmetric unit and the numbering scheme used in the tables. Thermal ellipsoids are drawn at 50% probability level (ORTEP-3 package[23]).

(12) Figgis, B. N. *Introduction to Ligand-Fields*; Interscience: London 1966; p 289.
(13) Shaw, W. H. R.; Bordeaux, J. J. *J. Am. Chem. Soc*. **1955**, *77*, 4729.

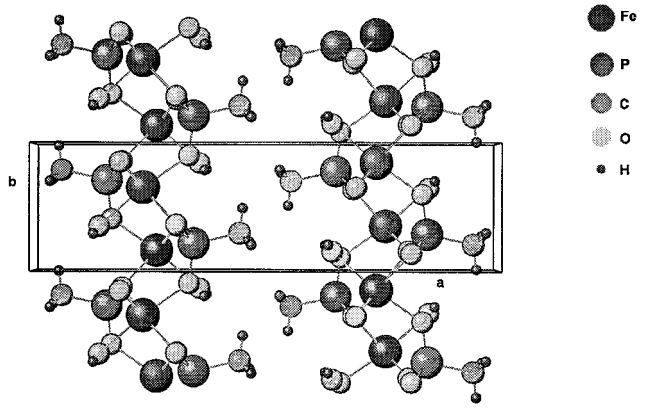

Figure 2. Unit-cell packing of $Fe[CH_3PO_3]\cdot H_2O$ viewed along the *c* axis.

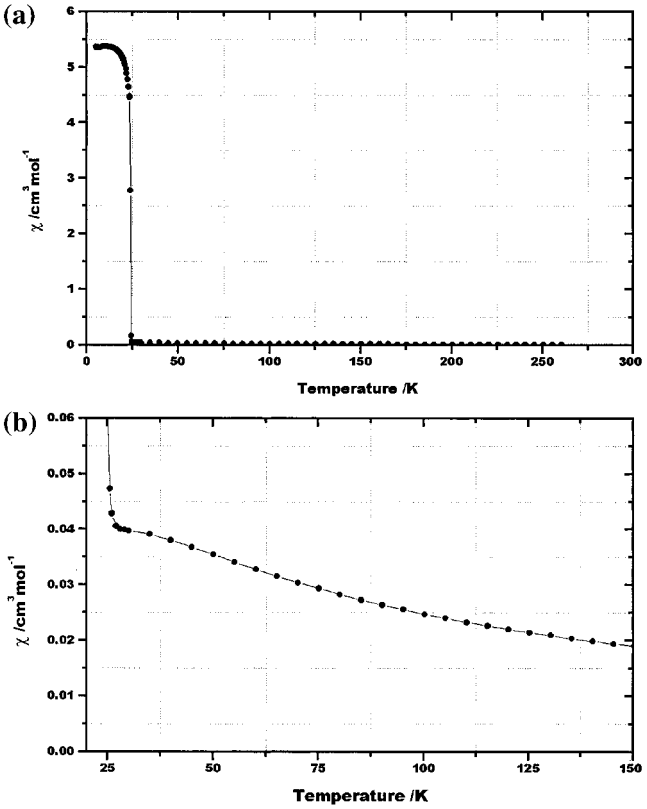

Figure 3. χ vs *T* plots of $Fe[CH_3PO_3]\cdot H_2O$ (a) in the temperature range 5−270 K and (b) in the temperature range 25−150 K.

nate, O(2), to form a kinked or crenelated (*ac*) layer. The P−C bond and the plane containing the methyl group are nearly perpendicular to the inorganic network between layers and the orientation of organic group is disordered. The slabs of neutral $Fe[CH_3PO_3]\cdot H_2O$ are then translationally related along the *a* axis of the unit cell with only van der Waals contacts between them.

Magnetic Properties. Magnetic susceptibility measurements were performed on a polycrystalline sample in the temperature range 5−270 K and in an applied field of 50 mT. The temperature dependence of molar magnetic susceptibility, χ_M, in the range 5−270 K, is shown in Figure 3a,b. Above 140 K, the magnetic behavior follows the Curie−Weiss law, and the Curie constant, *C*, is 3.99 $cm^3\cdot K\cdot mol^{-1}$. This corresponds to an effective magnetic moment of 5.65 μ_B, which is consistent with the presence of Fe(II) in a d^6 high-spin electronic configuration. This value is higher than that expected for the spin-only moment, i.e. 4.9 μ_B. The ^5D ($L = 2$) free-ion state of Fe(II) ion has orbital degeneracy, and in a cubic ligand-field, the ground state is the $^5T_{2g}$ state, with the lowest spin−orbit state $J = 1$.[12] A distortion in the $[FeO_6]$ site by the ligands causes a further splitting of the $J = 1$ state, and the resulting ground state can be either a singlet, $M_j = 0$, or doublet, $M_j = \pm 1$. Because the energy separation between the spin−orbit components in Fe(II) is of the order of 200 cm^{-1}, we expect an orbital contribution to the Fe(II) moment, which could explain the difference between the experimental and the spin-only values. The Weiss constant, i.e. $\Theta = -59$ K, indicates strong antiferromagnetic near-neighbor exchange interactions between the adjacent iron(II) ions. Below 100 K, the χ_M vs *T* plot shows a broad maximum centered at $T \sim 32$ K, with $\chi_{max} \sim 0.042$ cm^3/mol (see Figure 3b). On cooling, the susceptibility at $T = 25$ K sharply increases up to a maximum at $T \cong 24$ K and then decreases again. Field-cooled (FCM) and the zero-field-cooled (ZFCM) magnetizations in the 6−30 K temperature range were also measured, and the plot is reported in Figure 4. The ZFCM, obtained on cooling the sample in a zero field and then warming it in the field of 1000 Oe, shows a broad peak centered at $T \sim 24.5$ K. The FCM, obtained on cooling the sample within the same field of 1000 Oe, shows a rapid increase at $T = 25$ K, and then it start to be constant at $T \sim 13$ K down to the lowest measured $T = 6$ K. The temperature at the onset of the ZFC plot is taken as the critical temperature, T_N. Hysteresis loops at several temperatures below T_N have been measured, and those recorded at $T = 23$ K and at $T = 24$ K are reported in Figures 5 and 6, respectively. Below the critical temperature, all the hysteresis plots are similar and show that the magnetization is the sum of two contributions:

$$M(H,T) = M_{nc}(H,T) + \chi_{AFM}(T)H$$

Here $M_{nc}(H,T)$ is the uncompensated (ferromagnetic component) moment and χ_{AFM} is the antiferromagnetic susceptibility at the measuring temperature, *T*. M_{nc} was determined from the extrapolation to zero field of the linear part of the magnetization curve at high applied magnetic fields, and χ_{AFM}

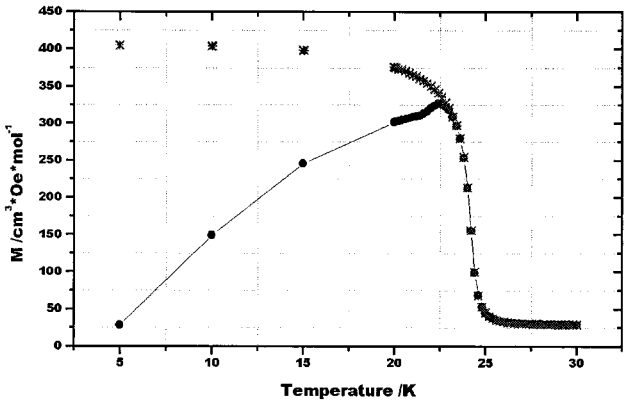

Figure 4. Temperature dependence of the ZFC (■) and FC (*) magnetization of $Fe[CH_3PO_3]\cdot H_2O$ below 30 K.

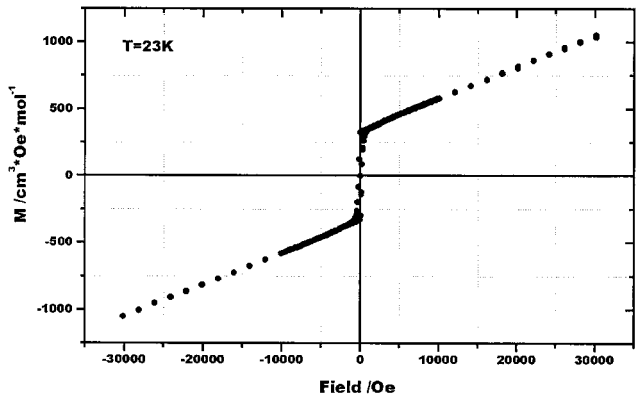

Figure 5. Hysteresis loop of Fe[CH_3PO_3]·H_2O measured at $T = 23$ K.

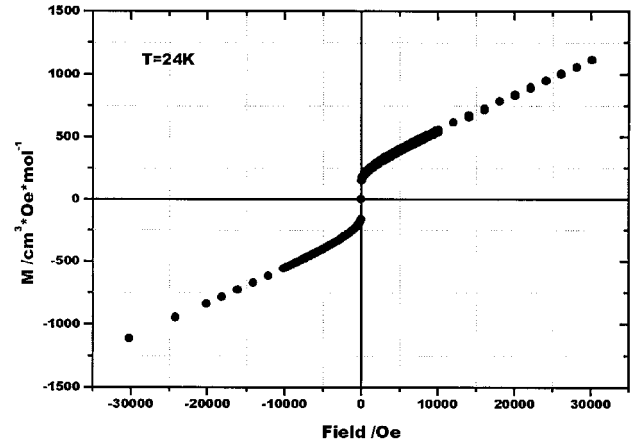

Figure 6. Hysteresis loop of Fe[CH_3PO_3]·H_2O measured at $T = 24$ K.

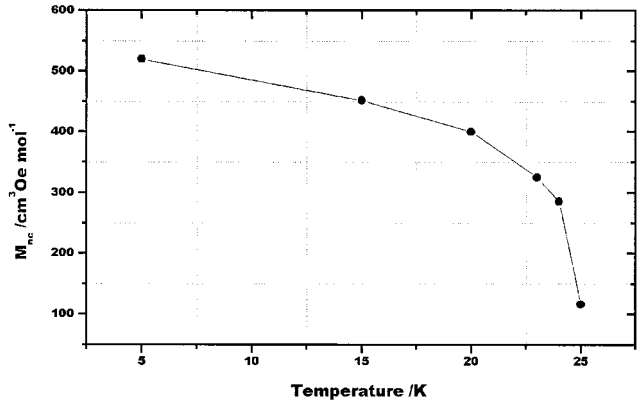

Figure 7. Temperature dependence of the uncompensated magnetization, M_{nc}, of Fe[CH_3PO_3]·H_2O in the region 5−25 K.

was determined as its slope. A temperature dependence of the uncompensated magnetization, M_{nc} (spontaneous magnetization), in the region 5−30 K has been plotted and is reported in Figure 7. The value of $M_{nc}(T)$ tends toward a value of 550 cm^3 Oe/mol, as $T \Rightarrow 0$ K, and it drops to zero as T approaches to the critical temperature, T_N. $M_{nc}(5)$ is substantially smaller than the value expected for the saturated magnetization of an $S = 2$ magnetic system, i.e ∼2.5% of it. Now, if we assume the uncompensated magnetization, M_{nc}, at the lowest measured temperature, i.e., $T = 5$ K to be $M_{nc}(0)$ and by using the following simple relation for the canting angle, α

$$\tan \alpha = M_{nc}(0)/g\mu_B S$$

we can estimate the angle $\alpha = 1.4°$. Hysteresis phenomena disappear at temperatures above T_N, where the isothermal magnetization vs field plot is linear. These results indicate definitely that the magnetic behavior of the compound is typical of a "weak ferromagnet" or "noncollinear antiferromagnet". The magnetic parameters of the title compound are reported in Table 3, together with those of the analogues taken from literature. The purely inorganic weak-ferromagnet (NH_4)[$Fe^{II}PO_4$]·H_2O[14] has also been included in the Table 3, because is lamellar and it possess the same metal−oxygen−phosphorus layer. In the unit cell the NH_4^+ ion lies in the interlayer region and the organic part of phosphonic groups are replaced by the phosphate oxygen. It is worth noticing that, along the series, similar values for the critical temperature T_N are observed, except for Fe(II) phenylphosphonate, where the 3D ordering temperature is slightly lower. The same trend has been observed in the series of Mn(II) phosphonates.[4,15]

Conclusions

Fe[CH_3PO_3]·H_2O represents an interesting example of a molecule-based "*weak ferromagnet*" or "*noncollinear antiferromagnet*". Single crystals were grown on warming slowly a sealed ampule, containing a filtered solution of the acid, urea, and iron(II) sulfate. The compound is stable to the air, and the crystal structure is lamellar, made of the inorganic layers alternating with the organic ones along the *a* axis of the unit cell. The former are made of Fe(II) octahedrally coordinated to the oxygens of the phosphonate ligand and to the water molecule, producing a cross-link Fe−O network. The octahedral symmetry around the iron(II) ions is highly distorted, and no inversion center between two adjacent metal ions is present. The organic layers are composed of methyl groups, bonded to the phosphorus atom of the ligand, and are pointed nearly perpendicular to the plane and away from the inorganic layer. They form bilayers with van der Waals contacts between them and are located above and below the inorganic sheets. The compound orders antiferromagnetically at $T_N = 25$ K, and the antiferromagnetism arises from interactions in the plane between nearest neighboring ions that take place via two different 180° Fe−O−Fe superexchange paths. The value of the $|T_N/\Theta|$ ratio is ∼0.4, (see Table 3), and this experimental finding is consistent with the 2D nature of the magnetic exchange. The molecular field, in fact, predicts $|T_N/\Theta| = 1$, but large deviations are expected for low-dimensional magnets, because of the short-range correlations above T_N. The estimation of *intra*planar superexchange value, *J*/*k*, can be done using the method of high-temperature expansion appropriate for a square planar

(14) Greedan, J. E.; Reubeunbauer, K.; Birchall, T.; Ehlert, M. *J. Solid State Chem*. **1988**, *77*, 376.
(15) (a) Fanucci, G. E.; Krzystek, J.; Meisel, M. W.; Brunel, L. C.; Talham, D. L. *J. Am. Chem. Soc*. **1998**, *120*, 5469. (b) Seip, C. T.; Granroth, G. E.; Meisel, M. W.; Talham, D. L. *J. Am. Chem. Soc*. **1997**, *119*, 7084.

Table 3. Magnetic Parameters of Fe(II) Phosphonates

compd	T_N/K	Θ/K	T_N/Θ	space group	*a*/Å	*b*/Å	*c*/Å	*β*/deg	interlayer spacing/Å	ref
$(NH_4)FePO_4$	26.0	−65	0.40	$Pmn2_1$	5.6656(1)	8.821(2)	4.8314(1)		8.82	14
$Fe[CH_3PO_3]H_2O$	25.0	−59	0.42	$Pna2_1$	17.538(2)	4.814(1)	5.719(1)		8.75	this work
$Fe[C_2H_5PO_3]H_2O$	24.5	−43	0.57	*Pn*	5.744(3)	10.33(1)	4.856(8)	91.0	10.33	9a
$Fe[C_6H_5PO_3]H_2O$	21.5	−56	0.38	$Pmn2_1$	5.669(8)	14.453(2)	4.839(7)		14.45	7
$Fe_2[O_3P(CH_2)_2PO_3]\cdot 2H_2O$	25.0	−52	0.48		5.67(1)	15.23(3)	4.82(1)		15.23	6

Heisenberg system for $S = 2$.[16] The position of the maximum in the χ vs T plot, $T(\chi_{max})$, is related to the *intra*planar exchange constant, J/k, by the relationships described by deJongh and Miedema:[17]

$$kT(\chi_{max})/|J|S(S+1) = 2.07 \quad (1)$$

and

$$[\chi_{max}|J|/Ng^2\mu_B{}^2] = 0.0547 \quad (2)$$

Two different J/k values were obtained using eqs 1 and 2, i.e. −2.6 and −2 K, respectively. These results indicate no agreement between the experimental data and the chosen model; the reason relies on the fact that the inorganic layers are crenelated and therefore the 2D Heisenberg square-planar model represents only a crude approximation. The analytical expression reported by Lines[16a] for a 2D Heisenberg square planar system from high-temperature expansion series and studied by Rushbrooke and Wood[16b] could not be used here, because of the sharp increase of the susceptibility below 25 K, which causes the 2D broad maximum to be not well-defined. The broad maximum in the χ vs T plot of $Fe[CH_3PO_3]\cdot H_2O$ appears at $T \sim 32$ K, and this value is ≈8 K higher than that observed in the corresponding $Mn[CH_3PO_3]\cdot H_2O$ ($S = 5/2$),[4,15] thus indicating the presence of a stronger near-neighbor antiferromagnetic exchange coupling in the Fe(II) compound. The two-dimensional nature of $Fe[CH_3PO_3]\cdot H_2O$ leads to a very small interlayer interaction J'/k. A 2D Heisenberg system requires some *inter*layer interactions J'/k to order 3-dimensionally. However, ordering in two-dimensions can also occur, if there is some anisotropy in the *in*-plane magnetic exchange and/or if there is sufficient single-ion anisotropy, and the Fe(II) ion has the single-ion anisotropy in this compound. Moreover, the critical temperatures, observed in the iron(II) phosphonate series, appear to have a little dependence on the interlayer spacing, (see Table 3) a trend which has been observed in the manganese analogues[15] and in some other layered hybrid organic−inorganic magnets.[15,17−19] By increase of the *inter*layer distance the interlayer exchange interaction J'/k ($d > 15$ Å) is even weaker, and so, probably the anisotropy is the driving force for the ordering transition in these Fe(II) phosphonates rather than the dipolar coupling or the interlayer superexchange. The change of phase from a low-dimensional antiferromagnetically coupled solid to a weakly ferromagnetic state is due to the "*spin-canting*".[8] In this situation the local spins in the ordered magnetic state are not perfectly antiparallel, leading to a net spontaneous magnetization, which saturates in a small field. Two mechanisms for producing the canted spin structure in these solids have been suggested: (1) single-ion magnetic anisotropy;[8,20] (2) the so-called antisymmetric Dzyaloshinsky−Moriya (DM) exchange coupling,[21] which may occur between neighboring centers and compete with isotropic Heisenberg antiferromagnetic exchange. The first mechanism operates when there are two equivalent sites of magnetic ions, but the directions of their anisotropy axes are different. DM mechanism acts to cant the spins, because the coupling energy is minimized when the two spins are perpendicular to each other. This coupling operates in addition to isotropic Heisenberg exchange, and it depends on the symmetry of the crystal (i.e. the interacting magnetic ions in the unit cell cannot be related by an inversion center of symmetry). Now, in $Fe[CH_3PO_3]\cdot H_2O$, the symmetry of the space group is $Pna2_1$ and it is low enough to allow the Dzyaloshinsky−Moriya exchange coupling to operate. Further, Fe(II) ion has a single-ion anisotropy, due to the spin−orbit coupling, so this generates the anisotropy in the g value. The antisymmetric exchange is then the origin for the canting of the spins, and the magnitude of the spontaneous magnetization depends on the canting angle. The DM mechanism has been suggested to operate in Mn(II) alkylphosphonates[4,15] and in the purely organic β-phase of the dithiadiazolyl radical.[22]

Acknowledgment. We acknowledge support from the Consiglio Nazionale delle Ricerche of Italy and European COST ACTION D14. C.B. thanks Mr. P. Filaci and Mr. C. Veroli for technical assistance.

Supporting Information Available: X-ray crystallographic file, in CIF format, for the structural determination of $Fe[CH_3PO_3]\cdot H_2O$. This material is available free of charge via Internet at http://pubs.acs.org.

IC0107126

(16) (a) Lines, M. E. *J. Phys. Chem. Solids* **1970**, *31*, 101. (b) Rushbrook, G. S.; Wood, P. J. *Mol. Phys.* **1963**, *1*, 257.
(17) DeJongh, J.; Miedema, R. *Adv. Phys*. **1974**, *23*, 64.
(18) Blake, A. B.; Hatfield, W. E. *J. Chem. Soc., Dalton Trans.* **1979**, 1725.
(19) (a) Reference 17, pp 108. (b) Bellitto, C.; Day, P. In *Comprehensive Supramolecular Chemistry*; Lehn, J. M., Ed.; Pergamon Press: New York, 1996; Vol. 7, pp 293−312.
(20) Moriya, T. *Phys. Rev.* **1960**, *117*, 635.
(21) Dzyaloshinsky, I. *J. Phys. Chem. Solids* **1958**, *4*, 241.
(22) Palacio, F.; Antorrena, G.; Castro, M.; Burriel, R.; Rawson, J.; Smith, J. N. B.; Bricklebank, N.; Novoa, J.; Ritter, C. *Phys. Rev. Lett*. **1997**, *79*, 2336.
(23) Farruga, L. J. *J. Appl. Crystallogr*. **1997**, *30*, 565.